Influence of *z/w* relation in Chill Block Melt Spinning (CBMS) process and analysis of thickness in ribbons

Marcelo R. Pagnola, Marcelo Barone, Mariano Malmoria and Hugo Sirkin
Fisica Capital Federal, INTECIN (UBA – CONICET), Buenos Aires, Argentina

Received 6 February 2014
Revised 27 May 2014
Accepted 8 July 2014

Abstract

Purpose – The purpose of this paper is to present an analysis over own and other authors data related to the process of Chill Block Melt Spinning (CBMS) and propose a model of analysis for interpreting.
Design/methodology/approach – The methodology used in this work is to present the data analyzed by other authors, organize own data similarly to establish comparison, and established models and propose a possible physical processes interpretation.
Findings – Similarity between own experimental data. with others data reported by other authors, both z/w ratio and the thicknesses of the films produced has been found. This allows us to establish an exponential decay of the parameters studied and possibly link it the Newtonian cooling to which the samples are subjected in its production.
Research limitations/implications – This work is the first model set up to predict dimensions in design process by CBMS as a function of parameters of the ribbon production process.
Practical implications – The prediction of the product dimensions, with adjusting the initial parameters, allows to improve the process of ribbon production, this saves tuning time of the machine and provides certainty in the molten material ejection.
Social implications – The efficient production of magnetic materials lets save efforts in the raw material process preparing in magnetic cores for the energy sector. This, improves production besides benefit society by the final product and the energy savings.
Originality/value – The value of this paper is to propose a model of analysis that allows standardize production parameters, and could even allow the use of these models in computer programs, process simulators in a more effective manner.

Keywords Solidification, Magnetic materials, Parameters, 2D modelling, Thin films
Paper type Research paper

1. Introduction

The casting rate is the main factor in the 3D problem of Chill Block Melt Spinning (CBMS) at the solidification stage, and this is regulated from the ejection orifice diameter (z) in the nozzle, and the mass conservation principle that determines the ribbon thickness (t) and width (w). The nozzle – copper wheel gap (G) is reported as another process value that takes stead in this technique. These parameters can be seen in Figure 1.

In conventional studies the rotational speed of the copper wheel varies for tangential speeds in the order of 5-40 m/s, with the other parameters fixed. At certain intervals of velocity it is obtained by CBMS as a final product, a ribbon of amorphous and/or nanocrystalline material, which depends on the composition used in the process. Usually, to obtain magnetic alloy ribbons, there are used: $Fe_{(x-y-n)}Si_{(y)}$ $B_{(n)}$and other

Multidiscipline Modeling in Materials and Structures
Vol. 11 No. 1, 2015
pp. 23-31

1573-6105
DOI 10.1108/MMMS-02-2014-0008

alloying minorities as Nb, Cu or Ti. Where (*y*) and (*n*) coefficients are between 9 and 15 percent at. respectively.

The *z*/*w* ratio decreases as the tangential velocity of the wheel (Wang, 2010) decreases as well; this can be seen in Figure 2.

Our studies show the obtained behavior Wang's and allow generalizing all the tests with a decreasing exponential function that varies for each of the studied cases.

2. Experimental development

2.1 Mother ingot preparation

An ingot mother (170 g) is obtained by 27.20 g of $Fe_{81}B_{19}$ (% wt) and 12.80 g of $Fe_{30}Si_{70}$ (% wt) of non-commercial alloys, and by the addition of 130 g of Fe in the form of granules. With these samples there is obtained an ingot with the following features:

$$[(\mathbf{Fe})\ 22.03\ \text{g} + (\mathbf{B})\ 5.17\ \text{g}] + [(\mathbf{Fe})\ 3.85\ \text{g} + (\mathbf{Si})\ 8.96\ \text{g}] + (\mathbf{Fe})\ 130\ \text{g} \rightarrow (\mathbf{Fe\,Si\,B})170\ \text{g} \quad (1)$$

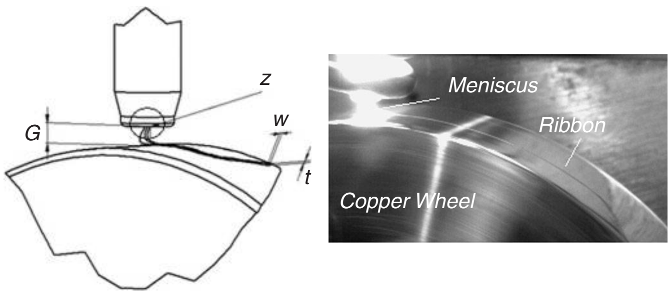

Figure 1.
CBMS process parameters

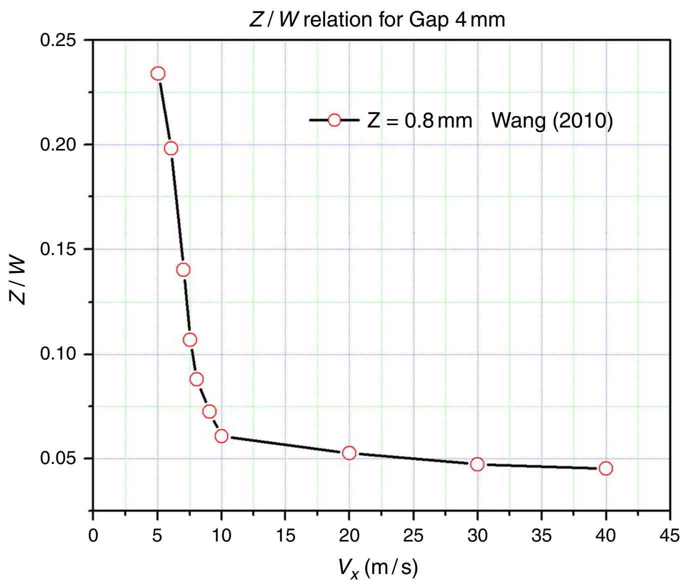

Figure 2.
Decreasing of *z*/*w* ratio with tangential velocity of the copper wheel in $Fe_{75}Si_{10}B_{15}$% at. amorphous ribbon, by Wang (2010)

$$(\mathbf{Fe})\ 155.88\ g + (\mathbf{Si})\ 8.96\ g + (\mathbf{B})\ 5.17\ g \rightarrow (\mathbf{Fe\ Si\ B})\ 170\ g \tag{2}$$

$$(\mathbf{Fe\ Si\ B}) \rightarrow \mathbf{Fe_{92}Si_5B_3}(\%Wt) \tag{3}$$

Then, we proceeded to vacuum-melt the first mother ingot in a specially designed graphite crucible. This procedure used a 7.5 kW induction furnace, Model RDO (LFI-7.5). The impurities in the non-commercial starting alloys: Al, C, Ca and S lower to 0.3% wt and the analysis of obtained composition is considered by Pagnola *et al.* (2014).

This procedure was repeated four times for the homogenization of the alloying elements. Using a temperature of 1,275°C, this is determined by the phase diagram and the corresponding proportion of the majority of the binary alloys (SGTE, 2004). This temperature is controlled by an optical pyrometer Micro-Epsilon brand and model CTLM 2HSF300-C3, mounted on a tripod and focused upon a graphite crucible.

2.2 Obtained ribbon

The obtained mother ingot has been milled to an average particle size of about 5 mm, and then placed inside a quartz tube of 10 mm diameter and 1.5 mm thick. This tube works as a crucible to obtain the ribbon. This crucible has a Boron Nitride nozzle attached with a circular (*z*) orifice in its center, through which flows the molten alloy.

The wheel works as a heat sink which reaches around one million degrees per second cooling rate (~10^6 K/s), necessary to achieve the glassy phase (Praisner *et al.*, 1995). The obtained method of ribbons is usually reported through the Melt Spinning process by different authors (Allia *et al.*, 1982; Muraca *et al.,* 2009). In Figure 1 it is shown the melt-spinning equipment, where it can be seen the small gap (*G*) between the ribbon and the casting wheel. The temperature profile is controlled by the external optical pyrometer to reaching a stabilization temperature zone for free jet ejection (Pagnola *et al.*, 2014).

Then, with an induction coil which heats the alloy over the melting point and argon overpressure, the alloy is expulsed through the nozzle at the ejection velocity on the high speed spinning wheel, reaching the casting rate. As a result, a continuous and mostly amorphous ribbon is obtained.

This procedure was repeated for wheel speeds between 5 and 40 m/s and gaps (*G*) of 2, 3 and 4 mm, and the *z*/*w* ratio was compared with the Wang's reference values, and the thickness (*t*) values with Tkatch *et al.* (2002), and Pozo Lopez *et al.* (2010). The obtained and fixed parameters of ribbon are plotted in Figure 3(a) and 3(b) All thicknesses and widths in the own production ribbons were measured as follows:

- For the width (*w*): it was used a Vernier type CALIBRE (Mitutoyo® brand) with 0.02 mm precision. Three parts of approximately 100 mm of each ribbon were selected. Then each of those parts was measured in five places and an average was obtained with the width values *w* (mm).
- For the thickness (*t*): it was used an external micrometer (Mitutoyo® brand), 0-25 mm with 0.01 mm precision. Three parts of approximately 100 mm of each ribbon were selected. Then each of those parts was measured in ten places and an average was obtained with the thickness values *t* (μm).

The values used in the gap are typical to identify this methodology as CBMS (Pavuna, 1981). Other estimates (Malmoria *et al.*, 2013) show that chemical composition in amorphous ribbon corresponds to $Fe_{78}\ Si_9\ B_{13}$ (%at.) within the estimated values.

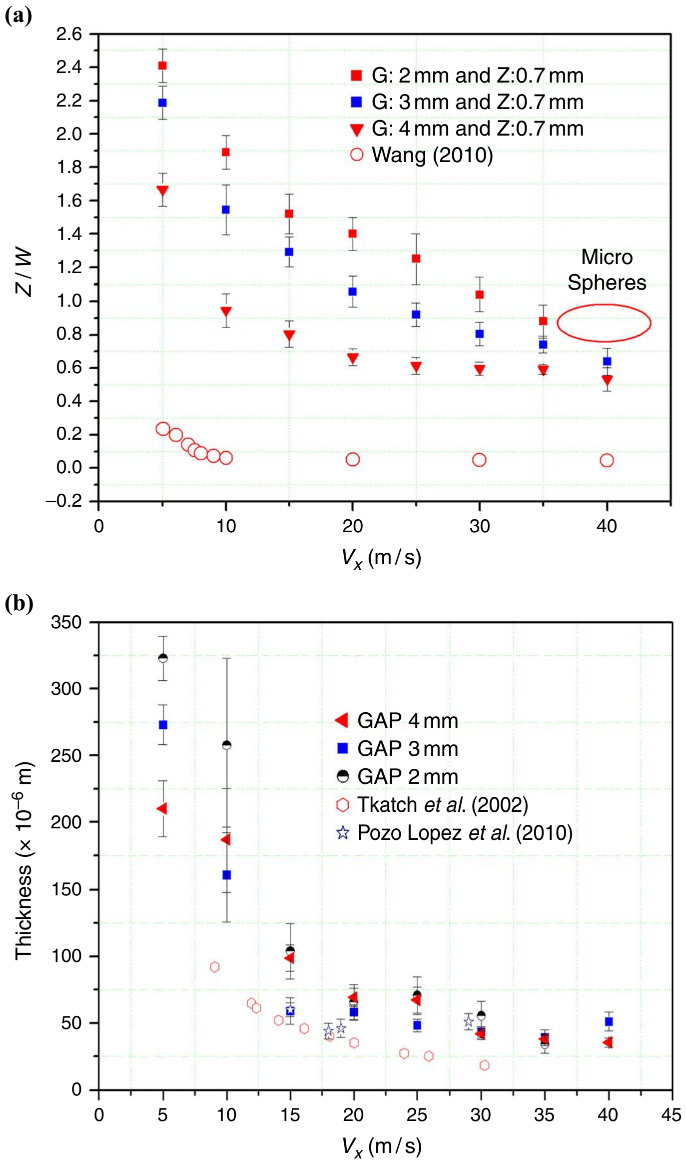

Figure 3.
(a) Comparative decreasing of *z/w* ratio with the tangential velocity of the copper wheel; (b) Comparative decreasing of ribbon thickness (*t*) with the tangential velocity of the copper wheel

3. Results and discussion

3.1 Results

With the values obtained Wang's in Figure 2 we can approximate the decay rate of the ratio *z/w* vs V_x as a decreasing exponential function with a correlation factor of R^2: 0.97273, as shown in Figure 4.

In Figure 3 there is shown that the shape of the decay of the *z/w* ratio for the measured values with gaps 2, 3 and 4 mm and orifice diameter (*z*) of 0.7 mm which were

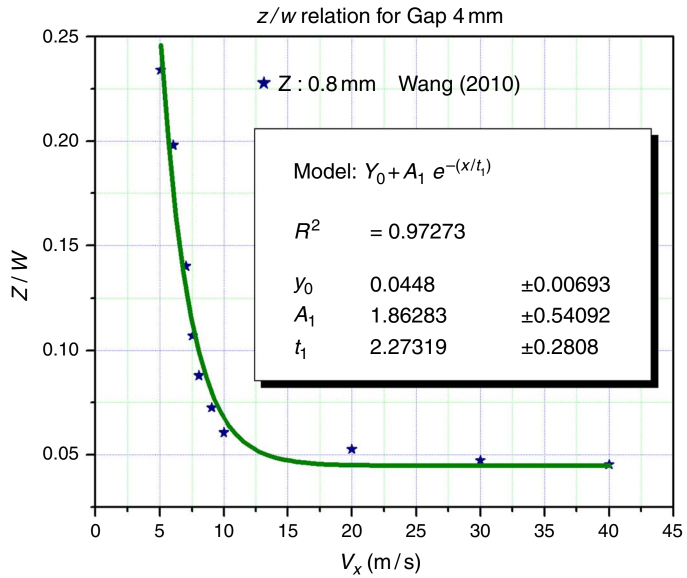

Figure 4. Decreasing exponential function for *z/w* ratio with the tangential velocity of the copper wheel V_x

obtained in our cases were similar to those of Wang (2010), except for a set of values between 35 and 40 m/s in the 2 mm gap curve. In this zone different diameter microspheres were obtained, without being able to observe a ribbon formation (see Figure 2). This common behavior allows us to propose the same decay function for our data, as follows:

- to 2 mm gap (*G*) and diameters of orifice (*z*) of 0.7 mm;
- to 3 mm gap (*G*) and diameters of orifice (*z*) of 0.7 mm; and
- to 4 mm gap (*G*) and diameters of orifice (*z*) of 0.7 mm.

3.2 General discussion

The aim of this work is to show that *z/w* relationship, widely used as a transforming factor between the 3D free jet and 2D simplification model, can approximate with an decreasing exponential function. The particular study of the parameters involved, and its intrinsic physics is the subject of another work. Therefore, analyzing the variation in the thickness (*t*) of the ribbons obtained in our production with relation to Tkatch *et al.* (2002) data (Figure 3(b)) we can observe a similar behavior in the decays. This allows us to adjust the values of Tkatch *et al.* (2002) with another function with the same decay, as displayed in Figure 8.

Applying the same method to the thicknesses (*t*) measured in our samples, there are obtained the values in Table I.

Both proposed decreasing exponential types, in *z/w* ratio and thickness (*t*) can be attributed to a beginning of influence the Newtonian cooling of mass in a convective medium such as atmospheric air due to the involved gaps in CBMS are larger than similar process as Planar Flow Casting (PFC) (Steen and Karcher, 1997). This is important factor in the competition between crystallization vs. amorphization and contact angle formation that occurs in this type of alloys in cast FeSiB ribbons

(Gibson and Delamore, 1988; Rivlin *et al.*, 1996). Also, due to increasing of the copper wheel speed (V_x) a greater amount of convective currents appears, and modifies the resultant heat-transfer coefficient on the adherence contact zone (h). Thereby, facilitating cooling and also fulfilling the principle of conservation of mass.

This described behavior may somehow be measured by calculating the Biot number (Equation (4)). In Table II this dimensionless number is calculated for values of copper wheel speed of 5 and 40 m/s and an average gap (G). In this table there is shown a growth of ~3.8 times in the action of convective forces with the V_x increasing copper wheel speed.

The characteristic length ($\boldsymbol{l}$) considered in Equation (4) is given by the obtained ribbon width ($\boldsymbol{w}$) and from the z/w ratios observed in Figure 3(a). The h and k values are considered on adherence contact zone to the wheel, and in the amorphous alloy, respectively (Liu *et al.*, 2009).

3.3 Particular discussion

- It was considered the z/w vs V_x relationship reported by Wang (2010) (Figure 2) for $Fe_{75}Si_{10}B_{15}$ (%at.) amorphous ribbons and an adjustment with decreasing exponential function with $R^2 = 0.97273$ (Figure 4) is proposed.
- It was observed an equal decreasing tendency in z/w vs V_x relationship in our $Fe_{78}Si_9B_{13}$ (% at.) amorphous ribbons samples (Figure 3(a)) produced with G: 2, 3 and 4 mm.
- It was proposed for our own samples produced with G: 2, 3 and 4 mm in z/w vs V_x relationship a decreasing exponential function. The parameters are reported in Figures 5-7, with $R^2 > 0.97$.
- The results on ribbons thickness (t) reported by Tkatch *et al.* (2002) and Lopez Pozo *et al.* (2010) (Figure 3(b)) were compared and we observed a thickness (t) vs V_x also decreasing exponential type that fits with $R^2 = 0.99324$ (Figure 8) for the

Table I. Decreasing exponential function parameters of ribbon thickness (t) given for our own production and other authors

	Model: $Y_0 + A_1 e^{-(x/t_1)}$ Y_0	A_1	t_1	R^2
Tkatch *et al.* (2002)	17.09175 ±2.41013	253.91703 ±26.70298	7.27046 ±0.66467	0.99324
Pozo Lopez *et al.* (2010)	I inconclusive values due to the narrow range of speeds used by the authors			
Gap 2	32.31694 ±4.72608	585.18306 ±85.89495	7.717 ±0.85515	0.89376
Gap 3	43.2559 ±2.40818	743.57447 ±148.0402	4.50135 ±0.49941	0.89254
Gap 4	26.85542 ±5.33854	318.04218 ±42.1972	10.57754 ±1.51522	0.95296

Table II. Biot number on contact zone in gap medium

	V_x (m/s)	
Equation (4)	5	40
$B_i = hl/k$	6.67×10^{-4}	2.58×10^{-3}

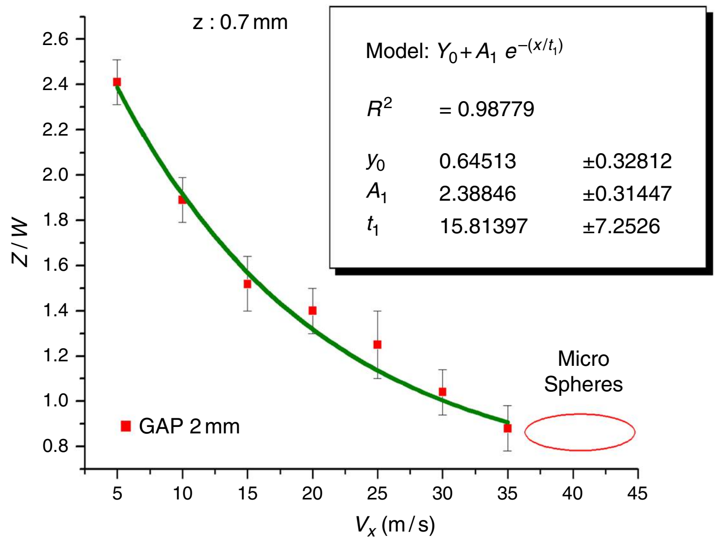

Figure 5. Decreasing exponential function for *z*/*w* ratio with the tangential velocity of the copper wheel and z: 0.7 mm

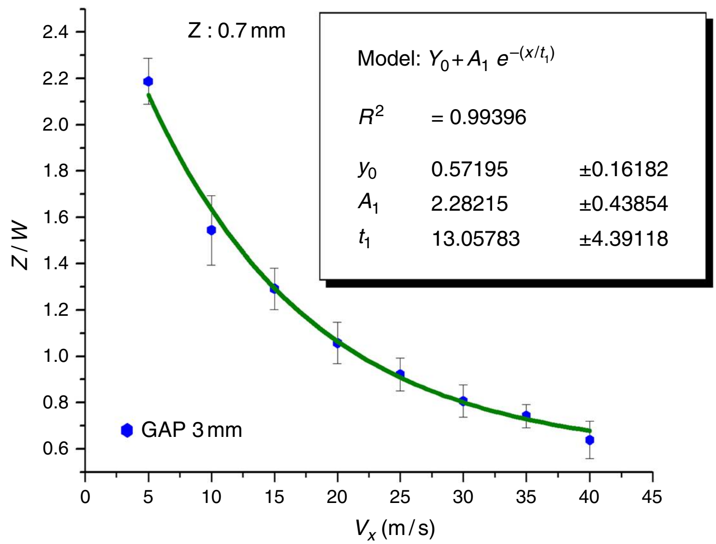

Notes: Gap 3 mm and z: 0.7 mm

Figure 6. Decreasing exponential function for *z*/*w* ratio with the tangential velocity of the copper wheel

first case. It is not conclusive on the latter case a decay as suggested in the first case, because of the narrow range of copper wheel speeds reported by the authors. While this data shows similar values to those reported for our samples in the velocity range between 15 and 30 m/s (Figure 3(b)).

A decreasing exponential in thickness (*t*) vs V_x is suggested for our own samples with *G*: 2.3 and 4 mm and their settings are perfectly correlated with the model proposed in Table I.

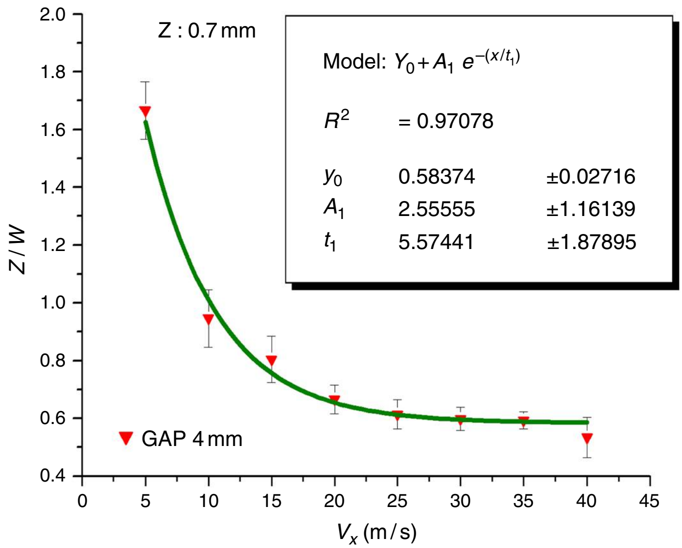

Notes: Gap 4 mm and z: 0.7 mm

Figure 7.
Decreasing exponential function for z/w ratio with the tangential velocity of the copper wheel

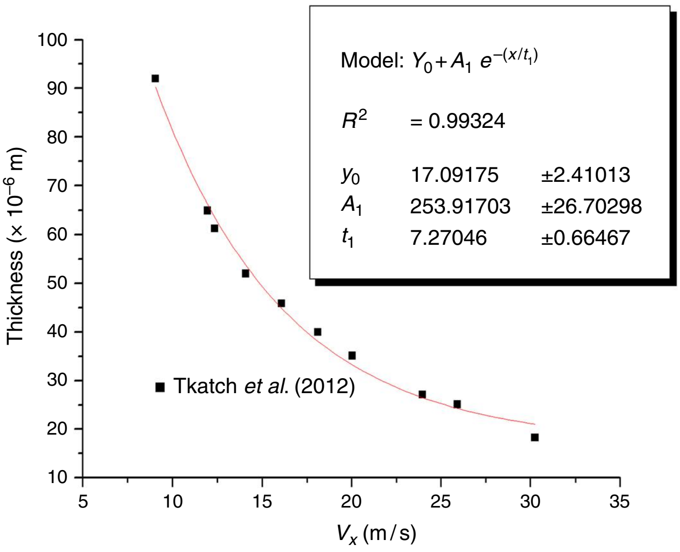

Figure 8.
Decreasing exponential function for ribbon thickness (t) with the tangential velocity of the copper wheel V_x

4. Conclusions

The decays proposed corresponds to the resultant heat-transfer coefficient on adherence contact zone (h) favors a Newtonian cooling in ribbons due to increased peripheral copper wheel speed (V_x), as shown in Table II by calculating the Biot number. This is valid due to the involved gaps in CBMS are larger that PFC, process where the effect of air on heat transport in negligibly small comparing to cooling towards the copper disk.

References

Allia, P., Milone, A.F., Vinai, F. and Fratucello, G. (1982), "Mössbauer spectroscopy of amorphous Fe-Si-8 alloys with different free volume content", *Journal of Applied Physics*, Vol. 53 No. 11, pp. 7750-7753.

Gibson, M.A. and Delamore, G.W. (1988), "Surface crystallization in melt-spun metallic glasses", *Journal of Materials Science*, Vol. 23 No. 4, pp. 1164-1170.

Liu, H., Chen, W., Qiu, S. and Liu, G. (2009), "Numerical simulation of initial development of fluid flow and heat transfer in planar flow casting", *Metallurgical and Materials Transactions B*, Vol. 40 No. 3, pp. 411-429.

Malmoria, M., Pagnola, M. and Barone, M. (2013), "Estudio Magnético de Cintas de FeSiB Obtenidas mediante Melt Spinning", *13° Congreso Internacional en Ciencia y Tecnología de Metalurgia y Materiales (SAM- CONAMET)*, Memory book, pp. 1-7.

Muraca, D., Silveyra, J., Pagnola, M. and Cremaschi, M. (2009), "Nanocrystals magnetic contribution to FINEMET type soft magnetic materials with Ge addition", *Journal of Magnetism and Magnetic Materials*, Vol. 321 No. 21, pp. 3640-3645.

Pagnola, M., Malmoria, M., Barone, M. and Sirkin, H. (2014), "Analysis of Fe_{78} Si_9 B_{13} (%at.) ribbons of noncommercial scrap materials produced by melt spinning equipment", *Multidiscipline Modeling in Materials and Structures*, Vol. 10 No. 4, pp. 511-524.

Pavuna, D. (1981), "Production of metallic glass ribbons by the chill-block melt spinning technique in stabilized laboratory conditions", *Journal of Materials Science*, Vol. 16 No. 9, pp. 2419-2433.

Pozo Lopez, G., Fabietti, L.M., Condo, A.M. and Urreta, S.E. (2010), "Microstructure and soft magnetic properties of Finemet-type ribbons obtained by twin-roller melt-spinning", *Journal of magnetism and Magnetic Materials*, Vol. 322 No. 20, pp. 3088-3093.

Praisner, T., Chen, J. and Tseng, A. (1995), "An experimental study of process behavior in planar flow melt spinning", *Metallurgical and Materials Transactions B*, Vol. 26 No. 1, pp. 1199-1208.

Rivlin, Z., Giang, H.G., Gibson, M.A., Froumin, N. and Baram, J. (1996), "Evaluation of the contact angle in rapid solidification by melt spinning", *Materials Science and Engineering*, Vol. A211 Nos 1-2, pp. 82-86.

SGTE (2004), "Alloy phase diagrams", available at: www.crct.polymtl.ca/FACT/phase_diagram.php?file=B-Fe.jpg&dir=SGTE,B-Fedatabase

Steen, P.H. and Karcher, C. (1997), "Fluid mechanics of spin casting of metals", *Annu. Rev. Fluid Mechanics*, Vol. 29 No. 1, pp. 373-397.

Tkatch, V.I., Limanovskii, A.I., Denisenko, S.N. and Rassolov, S.G. (2002), "The effect of the melt-spinning processing parameters on the rate of cooling", *Materials Science and Engineering*, Vol. A323 Nos 1-2, pp. 91-96.

Wang, C. (2010), *Numerical Modeling of Free Surface and Rapid Solidification for Simulation and Analysis of Melt Spinning*, Graduate theses and dissertations. Paper No. 11460, available at: http://lib.dr.iastate.edu.sci-hub.org/etd/11460

Corresponding author
Dr Marcelo R. Pagnola can be contacted at: mpagnola@gmail.com